DOI: 10.1002/anie.201000440

Imaging Agents

Bright Three-Photon Luminescence from Gold/Silver Alloyed Nanostructures for Bioimaging with Negligible Photothermal Toxicity**

Ling Tong, Claire M. Cobley, Jingyi Chen, Younan Xia, and Ji-Xin Cheng**

With more efficient penetration in biological tissues, near-infrared (NIR) excitation and/or emission between 1000 nm and 1350 nm opens a second window for in vivo imaging with low tissue autofluorescence.[1] Along with the development of red fluorescence proteins,[2] nanoparticles (NPs) have also been reported as imaging agents for multi-photon excitation microscopy. Examples include second harmonic generation (SHG) from ZnO nanowires[3,4] and nanorods,[5] third harmonic generation (THG) and four-wave mixing from Ag NPs,[6] Au NPs,[7] Au nanorods,[8,9] and NP antennas,[10] and multi-photon luminescence from Au nanorods,[11,12] Au NPs,[13,14] Au nanoshells,[15] and Au nanowires.[16,17] These intrinsic signals have enabled nanoscale imaging,[18] surface plasmon-mediated photolithography,[19] monitoring of the cellular uptake of NPs[20,21] and nanorods,[22] imaging of tumor cells in a matrix,[23] mapping the three-dimensional distribution of nanoshells in tumors,[15] and the probing of circulating nanorods in living animals.[24] Herein we present bright three-photon luminescence (3PL) from Au/Ag alloyed nanocages prepared by the galvanic replacement reaction.[25] With a large one-photon plasmon absorption cross-section, the nanocages have been demonstrated as a contrast enhancement agent in optical coherence tomography[26] and photoacoustic tomography,[27] and as a photothermal therapeutic agent in cancer treatment.[28] The plasmon field of nanocages has also been used for surface-enhanced Raman scattering.[29]

[*] C. M. Cobley, Dr. J. Chen, Prof. Y. Xia
Department of Biomedical Engineering, Washington University
Saint Louis, MO 63130 (USA)
Fax: (+1) 314-935-7448
E-mail: xia@biomed.wustl.edu
L. Tong, Prof. J.-X. Cheng
Department of Chemistry, Purdue University
West Lafayette, IN 47907 (USA)
Fax: (+1) 765-496-1902
E-mail: jcheng@purdue.edu
Prof. J.-X. Cheng
Weldon School of Biomedical Engineering, Purdue University
West Lafayette, IN 47907 (USA)

[**] This work was supported in part by an NSF grant (CBET-0828832) to J.X.C., an AHA predoctoral fellowship to L.T., and a 2006 NIH Director's Pioneer Award (DP1 OD000798) to Y.X.

Supporting information for this article, including details of metal nanostructure preparation, optical setup, cell culture, cell imaging, and tissue imaging, is available on the WWW under http://dx.doi.org/10.1002/anie.201000440.

We investigated the nonlinear optical (NLO) properties of Au/Ag nanocages using a multimodal multi-photon microscope.[30] By excitation with a femtosecond laser at 1290 nm, we observed a THG peak at 430 nm, together with a broad 3PL that is one order of magnitude stronger than that from pure Au or Ag NPs. 3PL with a similar profile and intensity was also observed in solid NPs made of a Au/Ag alloy. With the laser excitation far away from the plasmon resonance peaks of the alloyed nanostructures, the 3PL allowed for live cell imaging with undetectable photothermal toxicity.

The Au/Ag nanocages were synthesized using the galvanic replacement reaction as reported previously.[25] Two compositions were prepared by controlling the amount of $HAuCl_4$ added to the suspension of Ag nanocubes: 49% Ag/51% Au and 85% Ag/15% Au, where the atomic percentages were determined by energy-dispersive X-ray analysis (EDX). The extinction spectra (Figure 1a,b) revealed that the surface-plasmon resonance peaks of the two samples were located at 760 nm and 640 nm, respectively. Scanning electron microscopy (SEM) images showed that the two samples had similar dimensions (ca. 43 nm in edge length), with more pores on the surface of the first sample (see the insets for SEM images).

Using femtosecond laser excitation at 1290 nm and λ-scan imaging,[30] we recorded the NLO signals from Au/Ag nanocages spin-coated on a coverslip. We observed a THG peak at 430 nm, a SHG peak at 645 nm, and a broad luminescence in the visible region (Figure 1c). The NLO nature of the luminescence was confirmed by examination of the dependence of luminescence intensity on the excitation power. The luminescence signals were recorded as the incident beam power decreased from 8.3 mW to 2.4 mW at the sample and then increased accordingly. A cubic dependence of the signal intensity on the excitation power was observed (Figure 1d), which is indicative of a three-photon excitation process. No obvious intensity drop was observed when the excitation power returned to the same level, which demonstrates little photo-bleaching or photothermal degradation of the nanocages. Under the same conditions, pure Au nanospheres (Figure 1e), Ag nanocubes (Figure 1f), Ag nanospheres, and Au nanorods (Supporting Information, Figure S1) showed an intense THG peak at 430 nm and a very weak luminescence.

We compared the THG and 3PL signals quantitatively from Au/Ag nanocages, pure Au nanospheres, and pure Ag nanocubes. Under the same conditions, the THG intensity from Ag nanocubes was found to be the highest, followed by Au nanospheres and Au/Ag nanocages (Figure 2a–d). Significantly, the 3PL intensity from Au/Ag nanocages was about one order of magnitude higher than that from Au nano-

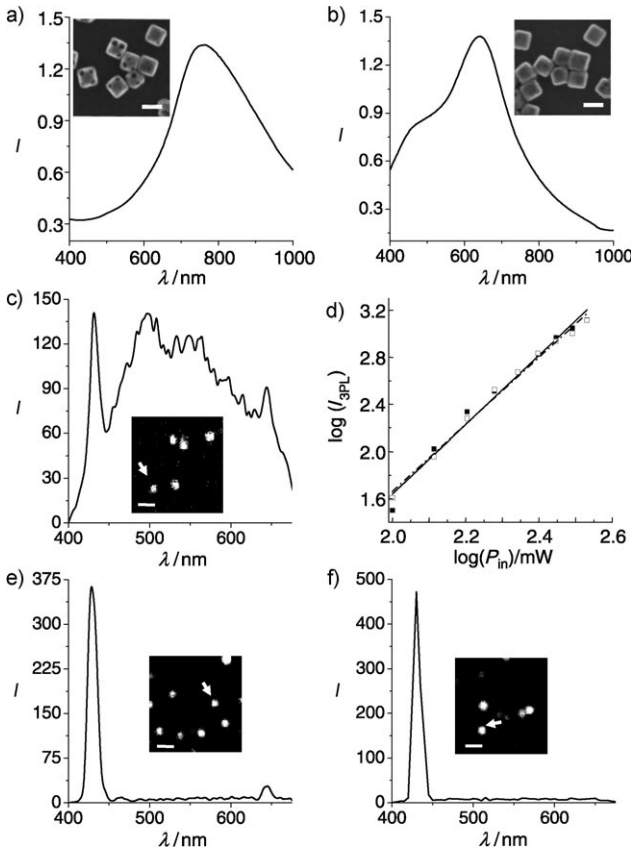

Figure 1. Third-harmonic generation (THG) and three-photon luminescence (3PL) from Au/Ag nanocages, Au nanospheres, and Ag nanocubes. a,b) Extinction spectra of Au/Ag nanocages with a) 49% Ag/51% Au and b) 85% Ag/15% Au. Inset: SEM images of the nanocages. Scale bars: 50 nm. c) Emission spectrum from a Au/Ag nanocage (49% Ag/51% Au) indicated by an arrow in the inset luminescence image, excited by a 1290 nm laser. d) Dependence of the luminescence intensity on the excitation power. The data was obtained by decreasing the excitation power from 8.3 mW to 2.4 mW, then increasing the power accordingly. Slopes: increasing (■,——): 2.94; decreasing (□,–•–•): 2.84. e) Emission spectrum from a 60 nm Au nanosphere (indicated by an arrow in the inset THG image). f) Emission spectrum from a Ag nanocube (40 nm in size) indicated by an arrow in the inset THG image. Scale bars in c, e, and f: 2 μm.

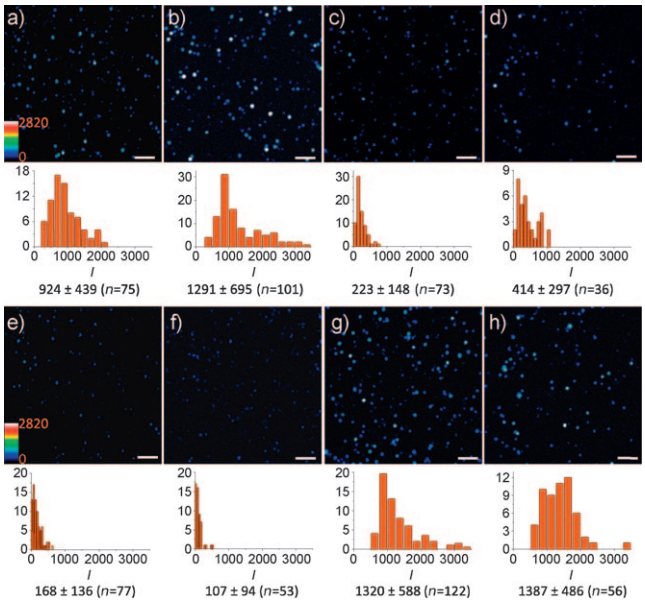

Figure 2. Quantitative comparison of THG and 3PL intensities from the Au/Ag nanocages, Au nanospheres, and Ag nanocubes, excited by a femtosecond laser at 1290 nm (laser power: 4.5 mW after objective). THG and 3PL images were acquired by an external detector with bandpass filters of 430/40 nm and 520/70 nm, respectively. a–d) THG images of a) 60 nm Au nanospheres, b) 40 nm Ag nanocubes, c) Au/Ag nanocages (49% Ag/51% Au), and d) Au/Ag nanocages (85% Ag/15% Au). e–h) 3PL images of e) Au nanospheres, f) Ag nanocubes, g) Au/Ag nanocages (49% Ag/51% Au), and h) Au/Ag nanocages (85% Ag/15% Au) in the same area used in (a–d). Scale bars: 5 μm. Intensity distributions are shown under each image.

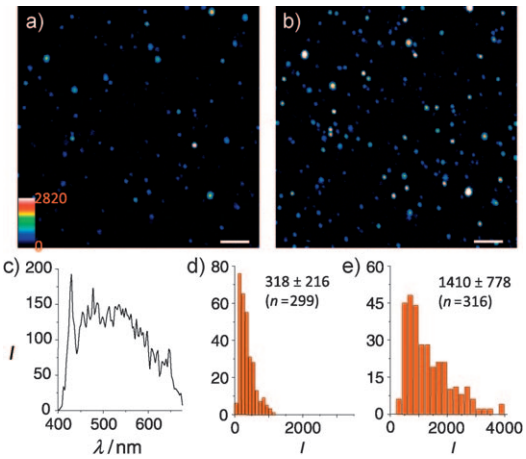

Figure 3. NLO properties of solid Au/Ag NPs (50% Ag/50% Au). a) THG and b) 3PL images of solid Au/Ag NPs spin-coated on a cover slip. Scale bars: 5 μm. c) Emission spectrum from a solid Au/Ag NP excited by a femtosecond laser at 1290 nm. d) THG intensity distribution and e) 3PL intensity distribution for the solid Au/Ag NPs.

spheres or Ag nanocubes (Figure 2e–h). Furthermore, we compared the two nanocage samples with different compositions. The nanocages with higher Ag content (Figure 2d) exhibited a stronger THG signal than the ones with lower Ag content (Figure 2c), whilst the 3PL intensities were at the same level (Figure 2g,h).

Because local E-field enhancement has been shown to arise from the pinholes on the surface of NPs,[31] we questioned whether the hollow and porous structure of nanocages contributed to the enhanced 3PL. To test such a possibility, we imaged solid NPs made of Au/Ag alloys by THG (Figure 3a) and 3PL (Figure 3b). Broad 3PL with a similar intensity profile to the nanocages was observed (Figure 3c). Both THG and 3PL signal intensities from the Au/Ag NPs (Figure 3d,e) were slightly higher than those from the Au/Ag nanocages with a similar composition (Figure 2c,g), which might be due to the larger volume of metal in the solid Au/Ag NPs than in the thin-walled nanocages. These results suggest that it is the Au/Ag alloy composition rather than the hollow and/or porous structure that contributed to the enhanced 3PL. In the alloyed nanostructures, Au and Ag atoms have been shown uniformly distributed.[32] A pair of Au

and Ag atoms could be considered as a dipole, and oscillation of the coupling dipoles may create a great field when exposed to laser irradiation. Therefore, in a microscopic view, the enhanced 3PL from Au/Ag nanocages and solid NPs could be ascribed to the interplay between Au and Ag at the atomic level.

Macroscopically, the luminescence excited by the 1290 nm laser could arise from a three-photon absorption process, followed by radiative transitions between excited electrons and holes. However, because the 1290 nm excitation is completely off the plasmon resonance, the three-photon absorption cross-section should be negligible compared to the parametric THG process, especially because Z-scan measurements have shown a larger third-order susceptibility from Au/Ag alloy nanoshells than pure Ag NPs.[33] With these considerations, we suggest an alternative mechanism for the enhancement of 3PL by which the generated THG photons might be re-absorbed by the same particle to produce the luminescence. This mechanism is supported by our observation of a weaker THG from Au/Ag alloyed nanostructures along with the enhanced 3PL. As additional supporting evidence, we were able to generate luminescence from the Au/Ag alloyed nanostructures using light at 430 nm (Supporting Information, Figure S2). Although both Au/Ag alloyed nanocages and solid NPs were found to display similar 3PL profiles, technically it is much easier to prepare Au/Ag alloyed nanocages with a wide range of tunable compositions and plasmon resonance peaks.[34] Therefore, we focused on the Au/Ag alloyed nanocages for the in vitro and ex vivo studies described below.

Similar to Au nanorods and nanoshells, Au/Ag nanocages also emit a two-photon luminescence (2PL).[35] The 2PL signal excited with a 0.6 mW femtosecond laser at 760 nm showed the same intensity level as the 3PL signal excited with a 4.3 mW femtosecond laser at 1290 nm (Supporting Information, Figure S3). Although the 2PL process is more efficient owing to the plasmon resonance enhancement, 3PL is advantageous over 2PL for cellular imaging in the phototoxicity aspect. In a plasmon resonant TPL process with nanorods or nanocages, a significant portion of the incident photons were absorbed by the plasma and converted into heat,[36,37] causing thermal degradation of the NPs[38,39] and damage to the surrounding tissues.[28,40–44] The thermal instability and photothermal toxicity make 2PL less attractive for bio-imaging. When the NIR excitation is off the plasmon resonance, as in the case of 3PL, the absorbed photons are more effectively used for generation of luminescence, either by three-photon absorption or by the parametric THG process. Consequently, much less thermal energy is produced in the 3PL process. We have compared the efficiency and photothermal toxicity of 2PL and 3PL experimentally for imaging Au/Ag nanocages in living cells. We incubated KB cells in a medium supplemented with Au/Ag nanocages for 12 h to allow cellular internalization. Two cells with similar density of nanocages were selected and illuminated by a 760 nm laser at 1.9 mW for 2PL imaging and a 1290 nm laser at 4.0 mW for 3PL imaging. As shown in Figure 4a,b, nanocages in cells could be visualized by both 2PL and 3PL (red) with the same level of intensity. To check the photothermal toxicity, we irradiated the KB cells by repetitive raster scanning of the same area. After 90 s scanning with the 760 nm laser, we observed membrane blebbing (ballooning bulges) and compromised integrity of plasma membrane as indicated by ethidium bromide staining, together with a reduced 2PL intensity from nanocages (Figure 4c). In contrast, neither damage to the plasma membrane nor reduction of 3PL intensity was observed during 90 s 3PL imaging (Figure 4d), even though a higher laser power was used in this study.

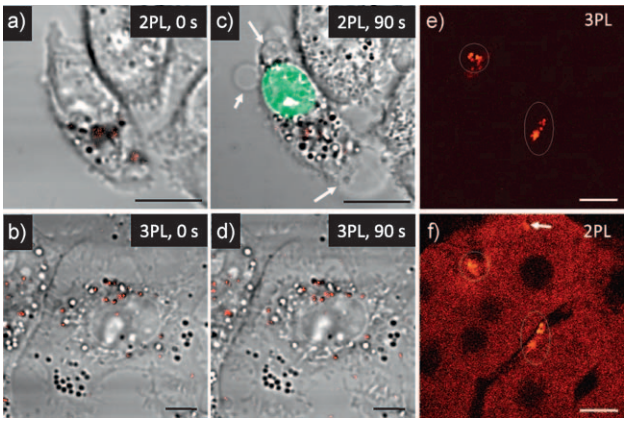

Figure 4. Comparison of 2PL and 3PL imaging of Au/Ag nanocages (49% Ag/51% Au) in KB cells (a–d) and liver tissues (e,f). a) 2PL image and b) 3PL image of Au/Ag nanocages (red) in KB cells before laser scanning. c) Image of the same cell as in (a) after scanning with 760 nm femtosecond laser for 90 s. Laser power after objective: 1.9 mW. After scanning, membrane blebbing (arrowed) and compromised membrane integrity indicated by ethidium bromide labeling (green) were observed. d) 3PL image of the same cell as in (b) after scanning with a 1290 nm femtosecond laser for 90 s. Laser power after objective: 4.0 mW. No morphological change or plasma membrane damage was observed. e) 3PL imaging of Au/Ag nanocages (white circles) in liver tissue. f) 2PL imaging in the same area as in (e). White arrow: Anomalously strong autofluorescence from tissue. Laser power after objective: 7 mW. Scale bars: 10 μm.

The 3PL further enabled us to map the distribution of intravenously injected Au/Ag nanocages in the liver of a mouse. The nanocages appeared as bright dots in the 3PL image of a sliced liver tissue (Figure 4e). Without autofluorescence background, the 3PL signal can potentially be used to determine the amount of nanocages deposited in the liver and other organs. In contrast, by femtosecond laser excitation at 760 nm, both nanocages and hepatocytes were simultaneously visualized by 2PL and two-photon excited autofluorescence, respectively (Figure 4f). The autofluorescence spot, indicated by the arrow in Figure 4f, made it difficult to selectively identify the nanocages.

In summary, we have shown that Au/Ag nanocages emit bright 3PL in the visible region when excited by a femtosecond laser at 1290 nm. The 3PL was one order of magnitude stronger than that from pure Au or Ag NPs. The enhancement was not due to the hollow and porous structure, but possibly due to the Au/Ag alloy composition. 3PL imaging showed little tissue autofluorescence background and exhibited undetectable photothermal toxicity because the NIR excitation laser was way off the plasmon resonance peak of

nanocages. The strong and intrinsic 3PL makes Au/Ag alloyed nanostructures a class of exciting NLO imaging agents for the study of trafficking of NPs in cells and bio-distribution of nanocarriers in small animals.

Received: January 25, 2010
Revised: March 2, 2010
Published online: April 6, 2010

Keywords: biosensors · luminescence · nanostructures · near-infrared imaging · photothermal toxicity

[1] A. M. Smith, M. C. Mancini, S. Nie, *Nat. Nanotechnol.* **2009**, *4*, 710.
[2] M. Drobizhev, S. Tillo, N. S. Makarov, T. E. Hughes, A. Rebane, *J. Phys. Chem. B* **2009**, *113*, 855.
[3] J. C. Johnson, H. Yan, R. D. Schaller, P. B. Petersen, P. Yang, R. J. Saykally, *Nano Lett.* **2002**, *2*, 279.
[4] K. Pedersen, C. Fisker, T. G. Pedersen, *Phys. Status Solidi c* **2008**, *5*, 2671.
[5] S. Kumar Das, M. Bock, C. O'Neill, R. Grunwald, K. M. Lee, H. W. Lee, S. Lee, F. Rotermund, *Appl. Phys. Lett.* **2008**, *93*, 181112.
[6] S. P. Tai, Y. Wu, D. B. Shieh, L. J. Chen, K. J. Lin, C. H. Yu, S. W. Chu, C. H. Chang, X. Y. Shi, Y. C. Wen, K. H. Lin, T. M. Liu, C. K. Sun, *Adv. Mater.* **2007**, *19*, 4520.
[7] M. Lippitz, M. A. van Dijk, M. Orrit, *Nano Lett.* **2005**, *5*, 799.
[8] Y. Jung, H. Chen, L. Tong, J.-X. Cheng, *J. Phys. Chem. C* **2009**, *113*, 2657.
[9] O. Schwartz, D. Oron, *Nano Lett.* **2009**, *9*, 4093.
[10] S. Palomba, M. Danckwerts, L. Novotny, *J. Opt. Pure Appl. Opt.* **2009**, *11*, 114030.
[11] H. Wang, T. B. Huff, D. A. Zweifel, W. He, P. S. Low, A. Wei, J.-X. Cheng, *Proc. Natl. Acad. Sci. USA* **2005**, *102*, 15752.
[12] K. Imura, T. Nagahara, H. Okamoto, *J. Phys. Chem. B* **2005**, *109*, 13214.
[13] R. A. Farrer, F. L. Butterfield, V. W. Chen, J. T. Fourkas, *Nano Lett.* **2005**, *5*, 1139.
[14] M. Eichelbaum, B. E. Schmidt, H. Ibrahim, K. Rademann, *Nanotechnology* **2007**, *18*, 355702.
[15] J. Park, A. Estrada, K. Sharp, K. Sang, J. A. Schwartz, D. K. Smith, C. Coleman, J. D. Payne, B. A. Korgel, A. K. Dunn, J. W. Tunnell, *Opt. Express* **2008**, *16*, 1590.
[16] H. Kim, C. Xiang, A. G. Güell, R. M. Penner, E. O. Potma, *J Phys Chem. C* **2008**, *112*, 12721.
[17] Q.-Q. Wang, J.-B. Han, D.-L. Guo, S. Xiao, Y.-B. Han, H.-M. Gong, X.-W. Zou, *Nano Lett.* **2007**, *7*, 723.
[18] Y. Nakayama, P. J. Pauzauskie, A. Radenovic, R. M. Onorato, R. J. Saykally, J. Liphardt, P. Yang, *Nature* **2007**, *447*, 1098.
[19] P. Zijlstra, J. W. M. Chon, M. Gu, *Nature* **2009**, *459*, 410.
[20] D. Nagesha, G. S. Laevsky, P. Lampton, R. Banyal, C. Warner, C. DiMarzio, S. Sridhar, *Int. J. Nanomed.* **2007**, *2*, 813.
[21] X. Qu, J. Wang, C. Yao, Z. Zhang, *Chin. Opt. Lett.* **2008**, *6*, 879.
[22] T. B. Huff, M. N. Hansen, Y. Zhao, J.-X. Cheng, A. Wei, *Langmuir* **2007**, *23*, 1596.
[23] N. J. Durr, T. Larson, D. K. Smith, B. A. Korgel, K. Sokolov, A. Ben-yakar, *Nano Lett.* **2007**, *7*, 941.
[24] L. Tong, W. He, Y. Zhang, W. Zheng, J.-X. Cheng, *Langmuir* **2009**, *25*, 12454.
[25] S. E. Skrabalak, L. Au, X. Li, Y. Xia, *Nat. Protoc.* **2007**, *2*, 2182.
[26] J. Chen, F. Saeki, B. J. Wiley, H. Cang, M. J. Cobb, Z.-Y. Li, L. Au, H. Zhang, M. B. Kimmey, Li, Y. Xia, *Nano Lett.* **2005**, *5*, 473.
[27] X. Yang, S. E. Skrabalak, Z.-Y. Li, Y. Xia, L. V. Wang, *Nano Lett.* **2007**, *7*, 3798.
[28] J. Chen, D. Wang, J. Xi, L. Au, A. Siekkinen, A. Warsen, Z.-Y. Li, H. Zhang, Y. Xia, X. Li, *Nano Lett.* **2007**, *7*, 1318.
[29] M. Rycenga, K. K. Hou, C. M. Cobley, A. G. Schwartz, P. H. C. Camargo, Y. Xia, *Phys. Chem. Chem. Phys.* **2009**, *11*, 5903.
[30] H. Chen, H. Wang, M. N. Slipchenko, Y. Jung, Y. Shi, J. Zhu, K. K. Buhman, J.-X. Cheng, *Opt. Express* **2009**, *17*, 1282.
[31] E. Hao, S. Li, R. C. Bailey, S. Zou, G. C. Schatz, J. T. Hupp, *J. Phys. Chem. B* **2004**, *108*, 1224.
[32] Y. Sun, Y. Xia, *J. Am. Chem. Soc.* **2004**, *126*, 3892.
[33] Z. Li, Y. Xue-Feng, F. Xiao-Feng, H. Zhong-Hua, L. Kai-Yang, *Chin. Phys. Lett.* **2008**, *25*, 1776.
[34] S. E. Skrabalak, J. Chen, Y. Sun, X. Lu, L. Au, C. M. Cobley, Y. Xia, *Acc. Chem. Res.* **2008**, *41*, 1587.
[35] L. Au, Q. Zhang, C. M. Cobley, M. Gidding, A. G. Schwartz, J. Chen, Y. Xia, *ACS Nano* **2010**, *4*, 35.
[36] S. Link, M. A. El-Sayed, *Int. Rev. Phys. Chem.* **2000**, *19*, 409.
[37] C.-H. Chou, C.-D. Chen, C. R. C. Wang, *J. Phys. Chem. B* **2005**, *109*, 11135.
[38] S. Link, Z. L. Wang, M. A. El-Sayed, *J. Phys. Chem. B* **2000**, *104*, 7867.
[39] H. Petrova, J. P. Juste, I. Pastoriza-Santos, G. V. Hartland, L. M. Liz-Marzan, P. Mulvaney, *Phys. Chem. Chem. Phys.* **2006**, *8*, 814.
[40] L. R. Hirsch, R. J. Stafford, J. A. Bankson, S. R. Sershen, B. Rivera, R. E. Price, J. D. Hazle, N. J. Halas, J. L. West, *Proc. Natl. Acad. Sci. USA* **2003**, *100*, 13549.
[41] H. Takahashi, T. Niidome, A. Nariai, Y. Niidome, S. Yamada, *Chem. Lett.* **2006**, *35*, 500.
[42] X. Huang, I. H. El-Sayed, W. Qian, M. A. El-Sayed, *J. Am. Chem. Soc.* **2006**, *128*, 2115.
[43] L. Tong, Y. Zhao, T. B. Huff, M. N. Hansen, A. Wei, J. X. Cheng, *Adv. Mater.* **2007**, *19*, 3136.
[44] R. S. Norman, J. W. Stone, A. Gole, C. J. Murphy, T. L. Sabo-Attwood, *Nano Lett.* **2008**, *8*, 302.

